Identifying Anisotropic Constraints in Multiply Labeled Bacteriorhodopsin by ^{15}N MAOSS NMR: A General Approach to Structural Studies of Membrane Proteins

A. James Mason,*[†] Stephan L. Grage,* Suzana K. Straus,* Clemens Glaubitz,[†] and Anthony Watts*

*Oxford University Biomembrane Structure Unit, Department of Biochemistry, Oxford OX1 3QU, United Kingdom; and [†]Centre for Biomolecular Magnetic Resonance and Institut für Biophysikalische Chemie, J. W. Goethe Universität, D-60439 Frankfurt, Germany

ABSTRACT   Structural models of membrane proteins can be refined with sets of multiple orientation constraints derived from structural NMR studies of specifically labeled amino acids. The magic angle oriented sample spinning (MAOSS) NMR approach was used to determine a set of orientational constraints in bacteriorhodopsin (bR) in the purple membrane (PM). This method combines the benefits of magic angle spinning (MAS), i.e., improved sensitivity and resolution, with the ability to measure the orientation of anisotropic interactions, which provide important structural information. The nine methionine residues in bacteriorhodopsin were isotopically ^{15}N labeled and spectra simplified by deuterium exchange before cross-polarization magic angle spinning (CPMAS) experiments. The orientation of the principal axes of the ^{15}N chemical shift anisotropy (CSA) tensors was determined with respect to the membrane normal for five of six residual resonances by analysis of relative spinning sideband intensities. The applicability of this approach to large proteins embedded in a membrane environment is discussed in light of these results.

INTRODUCTION

High-resolution structures of membrane and structural proteins and high molecular weight complexes are rare. Both membrane and structural proteins are difficult to crystallize. Membrane proteins are surrounded by lipids and may aggregate when removed from their normal environment, whereas structural proteins may have long filaments and may also aggregate. These same characteristics also hinder solution state NMR spectroscopy, which is not suitable for very large complexes due to the lack of fast isotropic tumbling needed for good spectral resolution. Solid-state NMR is not hindered by these technical problems and, in theory, can be readily applied to most systems to yield a variety of structural information. Although the complexity of NMR spectra increases with the molecular weight of protein complexes, solid-state NMR techniques have allowed a number of publications on high molecular weight proteins (Demura et al., 1998; Shon et al., 1991; Kim et al., 1998), and, in the case of bacteriorhodopsin (bR), orientational constraints have been obtained for singly labeled static oriented membrane samples (Ulrich et al., 1994, 1995; Moltke et al., 1998, 1999), and single distance measurements have been obtained between ^{13}C/^{13}C and ^{13}C/^{15}N labeled sites (Helmle et al., 2000; Griffiths et al., 2000).

A number of solid-state NMR approaches have been used to successfully study oriented membrane proteins and peptides. Static two-dimensional techniques (e.g., polarization inversion spin exchange at the magic angle (PISEMA) and heteronuclear correlation; Ramamoorthy et al., 1999) have been applied to obtain orientational information on the basis of the ^{15}N chemical shift and the [15]N-^{1}H dipolar interaction and have lead to the determination of the first three-dimensional structure of a membrane protein by solid-state NMR in the Protein Data Bank (1MAG.pdb; Ketchem et al., 1996). The resolution achievable in these experiments is, however, often limited and depends heavily on the degree of orientation of the membrane sample. Spectral overlap limits the numbers of residues that can be studied within the protein of interest. Magic angle sample spinning (MAS) can be used as an alternative method. It has the advantage that, in some cases, MAS yields better resolved and higher sensitivity spectra than the static approach, and individual residues of interest may be resolved and identified using MAS NMR methods. Due to the averaging of second rank tensor interactions, however, orientational information is lost when using MAS. Recently, it has been proposed to use a combined methodology, whereby MAS is used in conjunction with sample orientation. In the magic angle oriented sample spinning (MAOSS) approach (Glaubitz and Watts, 1998), the spinning frequency is chosen so as not to exceed the chemical shift anisotropy (CSA). As a result, the broad powder pattern transforms itself into a set of narrow, well resolved spinning sidebands around the isotropic chemical shift. The intensity of each of these sidebands depends on the size of the interaction tensor (Herzfeld and Berger, 1980; De Groot et al., 1991) and has an additional orientational dependence. This dependence allows the measurement of the tensor orientation with respect to the sample director. The application of MAOSS to a number of systems (Glaubitz

et al., 1999, 2000; Gröbner et al., 2000) has demonstrated the usefulness of this technique in answering structural questions for membrane proteins and peptides.

Here, selective ^{15}N labeling of a limited number of residues, all of one type (Fig. 1), permits multiple orientational constraints to be obtained for a set of residues from a protein in its membrane environment. The MAOSS technique is applied to resolve multiple resonances for specifically ^{15}N-methionine labeled bacteriorhodopsin in purple membranes (PM) and to determine the orientation of the principal axes of the ^{15}N chemical shift anisotropy tensors with respect to the membrane normal. Such a data set can form part of a set of constraints for structure modeling irrespective of the availability of any residue assignments (Marassi and Opella, 2003). The identification of individual residues within a multiply labeled sample and the determination of orientational constraints for each site will allow the use of specific labeling to follow key residues as reporters of structural and functional information within a biological membrane in a nonperturbing way, analogous to site directed mutagenesis approaches.

MATERIALS AND METHODS

Sample preparation

Halobacterium salinarium (S9) were cultured in a synthetic medium (1 L) containing all nutrients requisite for normal growth (Helgerson et al., 1992). ^{15}N-L-methionine (0.19 g/L) was added to the medium in place of the usual unlabeled L-methionine. After 5 days incubation (105 rpm, 37°C, in the dark), when the OD_{660} measurements had peaked, the cells were harvested and the purple membrane purified following published procedures (Oesterhelt and Stoeckenius, 1974). The purity of the prepared membrane was checked through spectrometry. Samples containing purified purple
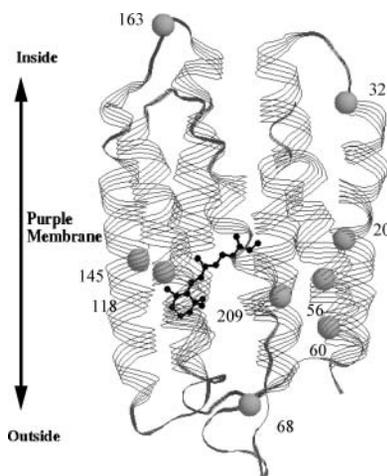
FIGURE 1 Bacteriorhodopsin three-dimensional structure indicating the positions of the nine ^{15}N labeled methionine residues, with six located in the transmembrane helices (Met-20, Met-56, Met-60, Met-118, Met-145, and Met-209), two in the loops (Met-68 and Met-163), and one (Met-32) at the loop helix interface of helix A. RASMOL was used with coordinates 2BRD from the Protein Databank, which is a structure of the protein embedded in the membrane (Grigorieff et al., 1996).

membrane (9.5 mg bR) were washed and resuspended in 5 mM Na_3Citrate, 5 mM KCl buffer (pH 6) prepared from water or deuterium hydroxide. For assignment purposes, bacteriorhodopsin single site mutant strain M20V was cultured as above except using ^{15}N-L-methionine labeled complex media (150 ml) (Helgerson et al., 1992).

To prepare oriented samples, the membranes (0.2 mg protein in 25 μl buffered D_2O for each plate, making a total of 9.5 mg bR) were spread evenly over 47 round, 0.07 mm thin glass plates with a diameter of 5.4 mm (Marienfeld GmbH, Lauda-Königshofen, Germany). Through controlled evaporation (91% humidity, room temperature, 2 days) these samples produced uniaxial films with good orientation of the purple membrane patches parallel to the sample plane. The plates were loaded into 7-mm Bruker (Karlsruhe, Gemany) MAS rotors and hydrated over a period of a few days by inverting the sealed rotors with a drop of saturated KNO_3 solution in the cap and alternately storing the rotor at 4° and 37°C. This process, as followed by static oriented ^{31}P spectroscopy, produces well-hydrated, oriented membranes that retain adhesion to the glass plates under MAS conditions. Powder samples were pelleted from distilled water and centrifuged into either 7-mm or 4-mm Bruker MAS rotors. Static oriented samples were produced similarly to the discs. A quantity of 0.4 mg protein in 120 μl distilled water was applied to 8-mm × 10-mm rectangular glass plates. Two applications were made and with 25 glass plates a total of 20 mg bacteriorhodopsin was prepared for static NMR experiments.

NMR experiments

Static NMR experiments were performed at 40.54 MHz for ^{15}N on a Bruker DSX 400 spectrometer, using a static probe. Cross-polarization (CP) experiments were performed at 253 K with 32-k acquisitions. A 200-Hz line broadening was applied to the free induction decays (FIDs) during processing. [15]N MAS and MAOSS experiments were performed at 40.54 MHz for ^{15}N on a Bruker Avance 400 equipped with 7-mm direct variable temperature-MAS probes. A recycle delay of 1 s was used with a contact time of 1 ms and an acquisition time of 48 ms. Optimized 80–100% ramped cross-polarization experiments using two pulse phase modulated (TPPM) decoupling (45-kHz ^{1}H field) were performed at 253 K at spinning frequencies of 2.5, 2.0, and 1.5 kHz. Samples were frozen before MAS was started to maintain sample stability under spinning conditions. The FIDs were processed with 8-k points and no line broadening before Fourier transformation. Processed spectra were deconvoluted to give sideband families for five resonances. For assignment purposes CPMAS spectra were acquired for purple membrane samples purified from both wild-type and single site mutant M20V. [15]N CPMAS experiments were performed at 60.82 MHz for ^{15}N on a Bruker Avance 600 equipped with 4-mm DVT-MAS probes. A recycle delay of 1 s was used with a contact time of 1 ms, an acquisition time of 49 ms, and a spectral width of 50 kHz. Optimized 80–100% ramped cross-polarization experiments again using two pulse phase modulated decoupling (62.5-kHz ^{1}H field) were performed at 253 K at a spinning frequency of 8 kHz. FIDs were processed with 16-k points and no line broadening before Fourier transformation. [15]N chemical shifts were measured relative to an external standard of solid $(NH_4)_2SO_4$ at 25 ppm.

Spectral simulation

In-house computer programs employing the GAMMA C++ library were used (Glaubitz and Watts, 1998) to compare the experimental spectra with spectra simulated for various ^{15}N CSA tensor orientations and mosaic spreads. The Floquet treatment (Levante et al., 1995) was used to obtain MAS spectra after successive rotations of the ^{15}N CSA tensor from its principle axis frame (PAS) first into the director frame (DF) (Fig. 2), with the z axis aligned along the local membrane normal. A second rotation from the director frame into the rotor fixed frame (RF) accounts for the mosaic spread and azimutal freedom in the uniaxially oriented sample, where a 3D-Gaussian distribution $\sim\sin(\beta_{DR}) \exp(-1/2 \beta_{DR}^2/\Delta\beta^2)$ was assumed for the
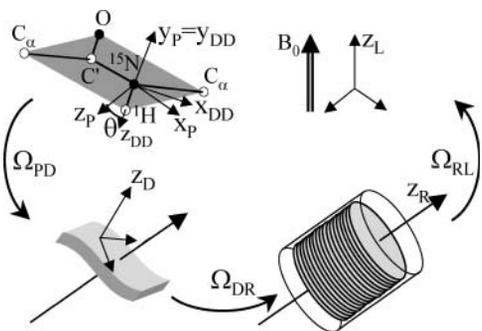
FIGURE 2 Definition of axes for ^{15}N CSA and ^{1}H-^{15}N dipolar coupling relative to the peptide plane in a ^{15}N labeled residue. The y axis for the dipolar tensor and σ_{22} CSA tensors are assumed to be collinear; therefore, the CSA→NH transformation is a rotation about the y_{DD} axis by an angle θ. The series of Euler angles that relate the membrane normal and the rotor long axis (Z_R) to the principal axis system of the ^{15}N CSA tensor are shown.

angle β_{DR} between director and rotor axis ($\Delta\beta$ measures the amount of mosaic spread), and an averaging over 5000 spectra was performed. A CSA value of $\sigma_{33} - \sigma_{iso} = 105.2$ ppm, based on the average value obtained from the MAS spectra, was employed for the simulations. The tensor element σ_{33} (least shielded) is aligned in the plane of the N–H bond and at an angle of around 16.6° for helical and for 13.9° for loop residues (Fushman et al., 1998) and is collinear with the z axis of the CSA principal axis system. The simulations are also sensitive to the asymmetry parameter η that was determined as $\eta = 0$ from the MAS spectrum that identifies the tensors as being approximately axially symmetric. Within the range $0 < \eta < 0.2$, however, no significant dependence of the simulated sideband patterns on η was observed. This way, MAOSS spectra for a single ^{15}N site were computed for β_{PD} ranging from 0° to 90° in steps of 2° and mosaic spread $\Delta\beta$ ranging from 0° to 30° in steps of 2°. They were compared to the isolated sideband pattern of each of the resolved lines of the experimental MAOSS spectrum, gained by fitting the respective peaks with Lorentzian lines. χ^2 values were used to quantify the difference between experimental data and simulation, and to obtain a best-fit value for the orientation β_{PD} and the mosaic spread $\Delta\beta$. A cutoff value for χ^2 of 10% above the respective χ^2 minimum was chosen to select the ranges for β_{PD} and $\Delta\beta$ in good agreement with the experimental data.

RESULTS

Resolution and assignments

Under static conditions the one-dimensional ^{15}N CP spectrum (Fig. 3) resolves resonances according to their orientation with respect to the magnetic field. The ^{15}N CSA is large and it is possible to separate resonances from loop or helices by nearly 200 ppm, although resolution between individual helical residues or between each of the two loop residues is poor.

Under the slow MAS conditions required for the MAOSS approach (Glaubitz and Watts, 1998), five resonances are clearly resolved in the isotropic central band for ^{15}N-L-methionine labeled purple membrane under MAS conditions (Fig. 4, *dotted line*) with three shoulders indicating a high probability of further resonances. The ^{15}N chemical shifts of these peaks are summarized in Table 1. Half height line widths vary from 65 to 80 Hz in the MAS powder sample, whereas in the MAOSS experiment the line widths are reduced to between 20 and 30 Hz. One resonance, at 119.8
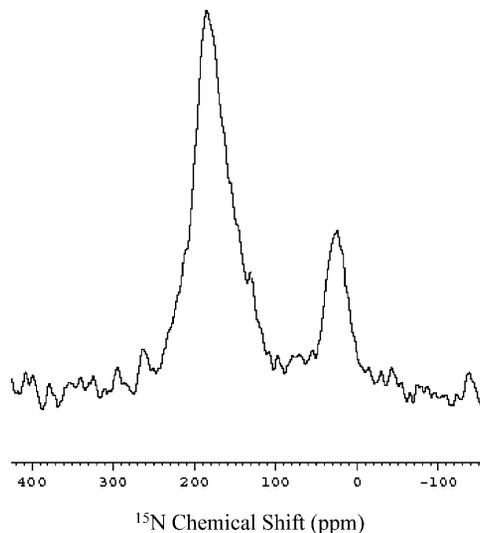
FIGURE 3 Static solid-state ^{15}N CP NMR spectrum (20 mg bR, 253 K, 32-k acquisitions, DSX 400) of ^{15}N-methionine labeled PM, oriented on glass plates at 0° with respect to B_0. The integral intensities are from 7 (180 ppm) to 2 (20 ppm), which would correspond to the seven helical residues and two loop residues of bacteriorhodopsin.

ppm, has almost double the half height line width of other resonances and may account for the ninth and last expected resonance. The methionine ^{15}N amide chemical shifts occupy a range of close to 10 ppm in this specifically labeled protein at 253 K. However, in spectra obtained from samples prepared from buffered water the contribution to the CPMAS spectral intensities from three resonances was low compared with other resonances. These shoulder resonances at 122.6, 122.0, and 120.9 ppm in the ^{15}N CPMAS spectrum could also not be resolved with sufficient clarity for sideband
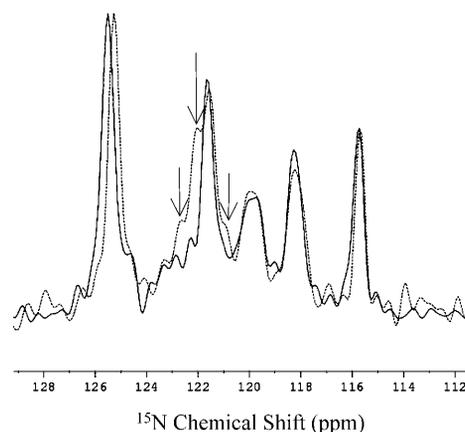
FIGURE 4 Small intensities that could not be clearly resolved in the spectrum of ^{15}N-methionine labeled bR in buffered H_2O under MAS conditions (*dotted line*) are removed by preparing MAOSS samples from buffered D_2O (*solid line spectrum*). Intensities corresponding to peaks (Fig. 4) that are removed in the presence of D_2O are indicated with arrows. Both spectra were acquired at 253 K and 5-kHz MAS frequency and show the centerband.

TABLE 1 Resolved isotropic chemical shifts and resonance line widths

^{15}N Chemical Shift (± 0.1 ppm)*				Full width at half height (± 1 Hz)†
MAS (600) (Fig. 7)	MAS (400) (Fig. 4)	MAOSS (ns)	MAOSS (D_2O) (Fig. 5)	
125.3	125.3	125.4	125.5 (A)	24
123.0	122.6	122.9	no	
122.2	122.0	nr	no	
121.6	121.6	121.6	121.6 (B)	21
no	120.9	120.9	no	
120.1	119.9	119.8	119.8 (C)	40
119.7	nr	nr	nr	
118.3	118.3	118.2	118.3 (D)	28
115.7	115.7	115.7	115.7 (E)	21

ns, not shown; no, not observed; nr, not resolved.
*Referenced to $(NH_4)_2SO_4$ at 25 ppm.
†Full line widths are measured at half resonance height for residual resonances in D_2O incubated MAOSS sample.

families to be obtained; hence samples incubated in buffered D_2O were used for MAOSS studies where these resonances were absent (Fig. 4, *solid line*).

The three MAOSS spectra acquired at only 400 MHz (proton frequency) for the sample prepared from buffered D_2O at spinning speeds that retain anisotropic information as spinning sidebands (Fig. 5) show that resolution obtained in the isotropic band is also obtained within the spinning sidebands. To analyze individual sideband families, spectra were deconvoluted and isolated sideband families were compared with simulated spectra. A χ^2 plot of β_{PD} against $\Delta\beta$ gives a clear minimum for the correct value of β_{PD}. An

example for resonance A is shown in Fig. 6 where a clear minimum corresponding to a mosaic spread of 18° and an angle for β_{PD} of 14°. Angular information for all five deconvoluted resonances is given in Table 2.

Assignment of the resonance attributable to Met-20 was obtained by comparing ^{15}N CPMAS spectra acquired at a greater MAS frequency for both wild-type membranes and for purple membranes prepared from *H. salinarium* strains containing the single site mutation M20V and grown on ^{15}N-L-methionine labeled media. The resultant spectrum (Fig. 7) shows a missing resonance corresponding to the mutated residue. The spectral subtraction makes this difference even clearer, whereas other small differences between the wild-type and mutant spectra are obscured below the noise. The resonance observed at 115.7 ppm in all other experiments was missing in this preparation and was assigned to the helical residue Met-20. The improved resolution obtained in this experiment also resolved two resonances at 120.1 and 119.7 ppm contributing to the one, broad resonance at 119.8 ppm in the MAOSS experiment.

DISCUSSION

The MAOSS NMR method described here has been developed in response to an increasing desire in the study of membrane protein structure and function to resolve multiple structural constraints from a membrane protein while still embedded in its bilayer environment.

Currently the method of choice for studying orientations in multiply labeled membrane peptides by NMR involves 2D
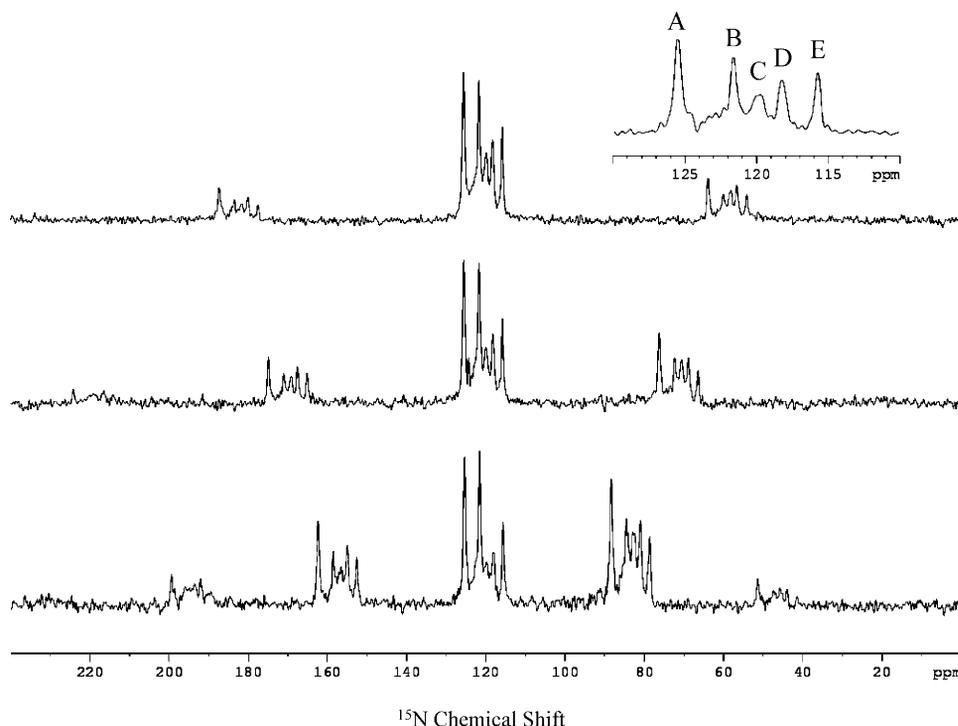
FIGURE 5 ^{15}N CP MAOSS spectra for ^{15}N-methionine labeled purple membranes prepared from buffered D_2O showing isotropic chemical shifts and spinning sideband families (9.5 mg bR, 253 K, 2.5- (*top*), 2- (*middle*), and 1.5-kHz (*bottom*) MAS frequencies; 160-, 132-, and 239-k acquisitions, respectively, DSX 400) for the five observed residual resonances. Analyses of the three spectra were combined to produce angle determinations for the five residual resonances (*inset, A–E*).
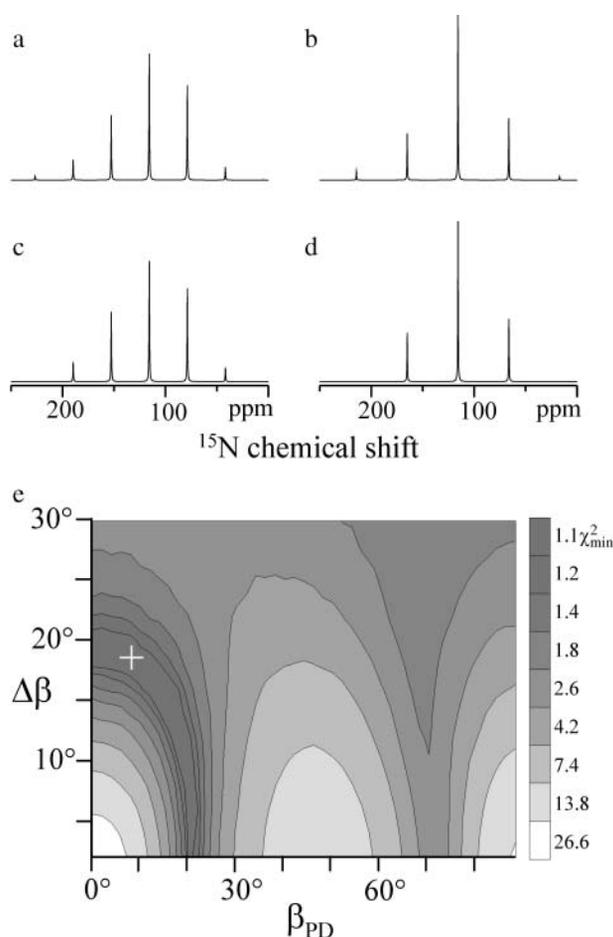
FIGURE 6 Illustration of the angle fitting process for resonance E. Simulated spectra (*top*) at 1.5-kHz spinning frequency (*a*) and 2 kHz (*b*) can be compared with spectra deconvoluted (*middle*) from the respective experimental data *c* and *d*. The difference between the experimental and simulated spectra (χ^2) over a range of angles for β_{PD} and mosaic spread ($\Delta\beta$) is plotted (*e*) and gives a clear minimum (+) for β_{PD} at 8° with mosaic spread of 18°.

FIGURE 7 Comparison of ^{15}N CPMAS NMR spectra obtained for wild-type (S9) (*top*) and M20V (*middle*) purple membranes labeled with ^{15}N-L-methionine (3 mg bR (S9), 2 mg bR (M20V); 253 K; 80–100% ramped CP; 8-kHz MAS frequency; Avance 600). The resonance at 115.7 ppm is absent as revealed in the spectral subtraction (*bottom*).

experiments applied to static oriented membrane films (Opella et al., 2002). In such experiments the specific orientation of an N–H bond, for example, is revealed by the dipolar or anisotropic chemical shift. The resolution obtainable is improved by performing experiments at increasing magnetic field strengths. Polarization inversion spin ex-

change at the magic angle is a more precise approach (assuming optimal experimental set up; Gan, 2000) than the MAOSS method proposed here, where signal intensities are measured, however the resolution available in the static experiment is limited by the size of the spectral line widths. For membrane proteins that do not orient so well on glass plates, such as in our experience larger proteins or those with considerable extramembrane domains (Gröbner et al., 1997), spectral overlap due to inhomogeneous line broadening is likely to hamper resolution of individual resonances from multiply labeled samples. This inhomogeneous line broadening is due to mosaic spread and is not improved by performing experiments at higher magnetic fields. In the MAOSS approach the spectral line widths are not dependent on mosaic spread, the major contributions to line broadening coming from insufficient averaging of dipolar couplings or intermediate motions on the NMR timescale. Thus for large proteins or proteins that have poor macroscopic orientation the MAOSS approach, in which slow spinning averages the mosaic spread, may be considered more suitable.

A further benefit of a MAS approach is the retention of the isotropic chemical shift information that is not observable in

TABLE 2   Angular constraints for resolved resonances

MAOSS resonance	β_{PD} (°)	Mosaic spread ($\Delta\beta$ (°))	Range of β_{PD} within 10% of χ^2 minimum (°)	Range of $\Delta\beta$ within 10% of χ^2 minimum (°)
A	16	18	0–22.5	9–24
B	4	14	0–16	5–15
C	34	14	31–47	9–20
D	28	4	27–29	0–7
E	8	18	0–22	0–21

static oriented samples. In this case, though assignment is usually a considerable problem in solid-state NMR, it is possible to use the isotropic chemical shifts of the resolved resonances to allow a comparison with samples containing single site mutations. Apart from the need to obtain protein samples other than wild type, the assignment is straightforward from the NMR data and was possible, under MAS conditions, using only very small quantities of labeled material (1–2 mg protein). The improved sensitivity of the MAS approach when compared with a standard static approach allows spectra to be acquired relatively quickly and on smaller quantities of labeled material. This is an important consideration when working with labeled membrane proteins that are typically not available in large amounts.

At relatively slow spinning frequencies (5 kHz) CPMAS NMR spectra of ^{15}N-methionine labeled purple membrane (Fig. 4) allow sufficient resolution of five resonances with a further three resonances appearing as shoulders. This resolution is significantly better than using simple 1D static oriented methods and reveals, in addition, the isotropic chemical shifts of the amide nitrogens. Similarly good resolution is obtained at slower spinning frequencies (2.5, 2.0, and 1.5 kHz) where, in addition, resonances in spinning sideband families can be resolved. Subsequent experiments at higher spinning speeds and magnetic field strength provide improved resolution, and two resonances can now be observed that give rise to only one broad resonance (C) in the MAOSS experiment (Fig. 7, *top*). The higher spinning frequencies (8 kHz) required for improved resolution in MAS prevent meaningful MAOSS spectra being acquired since the essential sidebands are removed; however, the information revealed by the complete resolution of all nine resonances is important for a number of reasons. Firstly, a total of nine peaks suggests that, as in previous studies (Seigneuret et al., 1991), the labeling was successful and that no significant scrambling of the ^{15}N label occurred. Secondly, complete resolution of the nine resonances is crucial in understanding the relative intensities attributable to different residues. Resonances from the nine methionine residues have significantly differing intensities in the 1D CPMAS (Fig. 4) spectra presented here. Further spectra were acquired over a range of temperatures and contact times and the intensities of the individual resonances varied (data not shown), likely due to the dependence of cross-polarization and heteronuclear decoupling efficiencies on molecular dynamics. The relatively poor sensitivity of ^{15}N spectroscopy restricted our experiments to conditions of optimal sensitivity for the five most intense resonances. CPMAS experiments performed with single site mutants of the two loop residues (M68K and M163C) have shown that resonance intensities attributable to these mutated residues are much lower in comparison with resonances from residues embedded in the transmembrane helices (Mason, 2001). Small reductions in intensity were seen in the region around 121 ppm in spectra acquired for membrane samples prepared from these mutants, and the subsequent removal of these small intensities in samples prepared from D_2O (Fig. 4) indicate that these resonances (122.6, 122.0, and 120.9 ppm) could be attributable to the three methionine residues on the surface of the protein (Met-32, Met-68, and Met-163) and that the residues themselves are not involved in hydrogen bonding. The intensities of these three resonances are too low for sideband families to be satisfactorily determined in samples prepared from buffered water, and so their contribution to the other, more intense resonances was removed by using samples prepared from buffered D_2O. In this process, membranes are suspended in buffered D_2O and rehydrated in a controlled D_2O atmosphere exposing amide protons from residues in loops at the surface of the protein to the aqueous environment. These amide protons are able to exchange with deuterons, whereas those that are buried in the membrane or, involved in secondary structure hydrogen bonding, remain protonated (Downer et al., 1986). Met-68 is shown in a high resolution electron diffraction structure of the surface of bacteriorhodopsin as being part of a β-sheet in the BC loop (Kimura et al., 1997); however, it is not involved in hydrogen bonding and infrared analysis of bacteriorhodopsin secondary structure has suggested the presence of disturbed β-structure (Downer et al., 1986). It is likely, therefore, that the amide proton of Met-68 can be exchanged in the presence of D_2O. The only other difference for the isotropic resonances between the MAOSS sample in D_2O and the MAS spectrum in H_2O was a very slight downfield shift of the resonance at 125.4 ppm. Such a shift was also observed, however, for MAOSS samples in H_2O (data not shown) and is not thought to be a result of deuterium exchange. The samples are frozen during the NMR experiments and further exchange does not occur over the 24-h period in which each spectrum is acquired. Since CPMAS uses magnetization transfer from protons to enhance the ^{15}N signal any residues that are now deuterated will be absent or significantly reduced from the resulting spectrum (Reif et al., 2001). Deuterium exchange performed on bacteriorhodopsin solubilized in *n*-dodecylmaltoside (Seigneuret and Kainosho, 1993) identified Met-32, Met-68, and Met-163 as being exchangeable on the basis of upfield shifts of the methionine [13]CO resonances attributed to these residues. These results are in agreement, therefore, with those presented here.

The good resolution obtained in the CP MAOSS experiment (Fig. 5) is vital in reducing errors and, with the exception of one resonance, there is little or no overlap of resonances. In the ^{15}N CP MAOSS spectrum six residual resonances are expected after treating the membranes in D_2O; however, only five resonances can be clearly resolved. From a comparison of resonance full widths at half height (FWHH; Table 1) for the resolved resonances it can be seen that resonance C at 119.8 ppm is unusually broad. In addition the data acquired at higher magnetic field strength and MAS

frequency (Fig. 7) reveals two peaks at 120.1 and 119.7 ppm that are not resolved in the MAOSS ^{15}N spectra, and hence it is clear that resonance C has a significant contribution from the sixth expected residual resonance.

χ^2 plots of the difference between spectra generated by computer simulations and those deconvoluted from the MAOSS spectra show, in each case, an easily identifiable minimum revealing the best fit for angles of β_{PD} and mosaic spread (See Fig. 6 for resonance E. The χ^2 plots for the remaining residues are included as supplementary data). A combination of spectra obtained at more than one spinning speed narrowed the region of possible angles and was found to be important to the data analysis. The low number of spinning sidebands available as a consequence of the employed magnetic field strength and operable spinning frequency, and hence low amount of inherent orientational information, would otherwise lead to only poorly defined χ^2 minima. Mosaic spread, a measure of the quality of orientations of the sample, is in the range of 14–18° for all but one residue. Variations in mosaic spread, from one site to another, is possible and is likely to be due to either variable conformational heterogeneity or motions in different regions of the protein. Resonance D has a best fit to a simulated spectrum with a much lower mosaic spread than would be expected. Increasing the mosaic spread though, in agreement with the other four resonances, does not change the solution for β_{PD}, and hence the reduced mosaic spread for this residue could be explained by reduced structural inhomogeneity in this region of the protein or, more likely, be an artifact arising from the narrow χ^2 minimum region.

Since we have sought to assign only one resonance in this study, a comparison of the determined structural constraints with available crystal structures is impracticable. The ability to identify numerous orientation constraints, however, has the potential to be used in a number of ways to obtain structural and functional information about membrane proteins. A data set as determined here could be used as part of an iterative modeling process, which, in combination with helix prediction programs and data sets from other labeled amino acids, could yield the backbone structure of a membrane embedded protein. The number of solvent accessible residues can also be assessed by the methods described here, and individual resonances can be assigned. The ability to resolve, select, and assign resonances from selectively labeled membrane proteins and obtain structural information as described for methionine 20, provides a valuable tool box for the membrane protein biophysicist. The resolution obtained renders MAOSS, in combination with specific labeling, a useful technique in the study of conformational changes at the molecular level and increases the applicability of structural solid-state NMR experiments to membrane proteins. Further improvements and adaptations of this technique are underway in our laboratories with a view to increasing the range of information that can be obtained and proteins that can be studied.

REFERENCES

De Groot, H. J. M., S. O. Smith, A. C. Kolbert, J. M. L. Courtin, C. Winkel, J. Lugtenburg, J. Herzfeld, and R. G. Griffin. 1991. Iterative fitting of magic angle spinning NMR spectra. *J. Magn. Reson.* 91:30–38.

Demura, M., M. Minami, T. Asakura, and T. A. Cross. 1998. Structure of *Bombyx mori* silk fibroin based on solid state NMR orientational constraints and fiber diffraction unit cell parameters. *J. Am. Chem. Soc.* 129:1300–1308.

Downer, N. W., T. J. Bruchman, and J. H. Hazzard. 1986. Infrared spectroscopic study of photoreceptor membrane and purple membrane. Protein secondary structure and hydrogen deuterium exchange. *J. Biol. Chem.* 261:3640–3647.

Fushman, D., N. Tjandra, and D. Cowburn. 1998. Direct measurement of ^{15}N chemical shift anisotropy in solution. *J. Am. Chem. Soc.* 120:10947–10952.

Gan, Z. 2000. Spin dynamics of polarization inversion spin exchange at the magic angle in multiple spin systems. *J. Magn. Reson.* 143:136–143.

Glaubitz, C., I. J. Burnett, G. Gröbner, A. J. Mason, and A. Watts. 1999. Deuterium-MAS NMR spectroscopy on oriented membrane proteins: applications to photointermediates of bacteriorhodopsin. *J. Am. Chem. Soc.* 121:5787–5794.

Glaubitz, C., G. Gröbner, and A. Watts. 2000. Structural and orientational information of the membrane embedded M13 coat protein by 13 C-MAS NMR spectroscopy. *Biochim. Biophys. Acta.* 1463:151–161.

Glaubitz, C., and A. Watts. 1998. Magic angle-oriented sample spinning (MAOSS): a new approach toward biomembrane studies. *J. Magn. Reson.* 130:305–316.

Griffiths, J. M., A. E. Bennett, M. Engelhard, F. Siebert, J. Raap, J. Lugtenburg, J. Herzfeld, and R. G. Griffin. 2000. Structural investigation of the active site in bacteriorhodopsin: geometric constraints on the roles of Asp-85 and Asp-212 in the proton pumping mechanism from solid state NMR. *Biochemistry.* 39:362–371.

Grigorieff, N., T. A. Ceska, K. H. Downing, J. M. Baldwin, and R. Henderson. 1996. Electron-crystallographic refinement of the structure of bacteriorhodopsin. *J. Mol. Biol.* 259:393–421.

Gröbner, G., I. J. Burnett, C. Glaubitz, G. Choi, A. J. Mason, and A. Watts. 2000. Observations of light-induced structural changes of retinal within rhodopsin. *Nature.* 405:810–813.

Gröbner, G., A. Taylor, P. T. F. Williamson, G. Choi, C. Glaubitz, J. A. Watts, W. J. de Grip, and A. Watts. 1997. Macroscopic orientation of natural and model membranes for structural studies. *Anal. Biochem.* 254:132–136.

Helgerson, S. L., S. L. Siemen, and E. A. Dratz. 1992. Enrichment of bacteriorhodopsin with isotopically labelled amino acids by biosynthetic incorporation in *Halobacterium halobium. Can. J. Microbiol.* 38:1181–1185.

Helmle, M., H. Patzelt, A. Ockenfels, W. Gärtner, D. Oesterhelt, and B. Bechinger. 2000. Refinement of the geometry of the retinal binding pocket in dark-adapted bacteriorhodopsin by heteronuclear solid-state NMR distance measurements. *Biochemistry.* 39:10066–10071.

Herzfeld, J., and A. E. Berger. 1980. Sideband intensities in NMR spectra of samples spinning at the magic angle. *J. Chem. Phys.* 73:6021–6040.

Ketchem, R. R., K. C. Lee, S. Huo, and T. A. Cross. 1996. Macromolecular structural elucidation with solid-state NMR-derived orientational constraints. *J. Biomol. NMR.* 8:1–14.

Kim, Y., K. Valentine, S. J. Opella, S. L. Schendel, and W. A. Cramer. 1998. Solid-state NMR studies of the membrane-bound closed state of the colicin E1 channel domain in lipid bilayers. *Protein Sci.* 7:342–348.

Kimura, Y., D. G. Vassyiyev, A. Miyazawa, A. Kidera, M. Matsushima, K. Mitsuoka, K. Murata, H. Terushisa, and Y. Fujiyoshi. 1997. High resolution structure of bacteriorhodopsin determined by electron crystallography. *Photochem. Photobiol.* 66:764–767.

Levante, T. O., M. Baldus, B. H. Meier, and R. R. Ernst. 1995. Formalized quantum mechanical floquet theory and its application to sample spinning in nuclear magnetic resonance. *Mol. Phys.* 86:1195–1212.

Marassi, F. M., and S. J. Opella. 2003. Simultaneous assignment and structure determination of a membrane protein from NMR orientational restraints. *Protein Sci.* 12:403–411.

Mason, A. J. 2001. Solid state NMR studies of bacteriorhodopsin and the purple membrane. PhD thesis. University of Oxford, Oxford, UK.

Moltke, S., A. A. Nevzorov, N. Sakai, I. Wallat, C. Job, K. Nakanishi, M. P. Heyn, and M. F. Brown. 1998. Chromophore orientation in bacteriorhodopsin determined from the angular dependence of deuterium nuclear magnetic resonance spectra of oriented purple membranes. *Biochemistry.* 37:11821–11835.

Moltke, S., I. Wallat, N. Sakai, K. Nakanishi, M. F. Brown, and M. P. Heyn. 1999. The angles between the C1-, C5-, and C9-methyl bonds of the retinylidene chromophore and the membrane normal increase in the M intermediate of bacteriorhodopsin: direct determination with solid-state ^{2}H NMR. *Biochemistry.* 38:11762–11772.

Oesterhelt, D., and W. Stoeckenius. 1974. Isolation of the cell membrane of *Halobacterium halobium* and its fractionation into red and purple membranes. *Methods Enzymol.* 31:667–678.

Opella, S. J., A. Nevzorov, M. F. Mesleh, and F. M. Marassi. 2002. Structure determination of membrane proteins by NMR spectroscopy. *Biochem. Cell Biol.* 80:597–604.

Ramamoorthy, A., C. H. Wu, and S. J. Opella. 1999. Experimental aspects of multidimensional solid-state NMR correlation spectroscopy. *J. Magn. Reson.* 140:131–140.

Reif, B., C. P. Jaroniec, C. M. Rienstra, M. Hohwy, and R. G. Griffin. 2001. H-H MAS corrrelation spectroscopy and distance measurements in a deuterated peptide. *J. Magn. Reson.* 151:320–327.

Seigneuret, M., and M. Kainosho. 1993. Localisation of methionine residues in bacteriorhodopsin by carbonyl ^{13}C-NMR with sequence-specific assignments. *FEBS Lett.* 327:7–12.

Seigneuret, M., J. M. Neumann, D. Levy, and J. L. Rigaud. 1991. High-resolution ^{13}C NMR study of the topography and dynamics of methionine residues in detergent solubilised bacteriorhodopsin. *Biochemistry.* 30:3885–3892.

Shon, K.-J., Y. Kim, L. A. Colnago, and S. J. Opella. 1991. NMR studies of the structure and dynamics of membrane-bound bacteriophage Pf1 coat protein. *Science.* 252:1303–1308.

Ulrich, A. S., I. Wallat, M. P. Heyn, and A. Watts. 1995. Re-orientation of retinal in the M-photointermediate of bacteriorhodopsin. *Nat. Struct. Biol.* 2:190–192.

Ulrich, A. S., A. Watts, A. Wallat, and M. P. Heyn. 1994. Distorted structure of the retinal chromophore in bacteriorhodopsin resolved by ^{2}H-NMR. *Biochemistry.* 33:5370–5375.